Original Article
Synthesis and assessment of ZD2-(68Ga-NOTA) specific to extradomain B fibronectin in tumor microenvironment for PET imaging of pancreatic cancer

Songqi Gao[1,4*], Jingcan Qin[1*], Olga Sergeeva[2], Maxim Sergeev[3], Peter Qiao[1], Sarah Roelle[1], Norbert Avril[2,3], Zhenghong Lee[2], Yajuan Li[4], Zhengrong Lu[1,2]

*Departments of [1]Biomedical Engineering, [2]Radiology, Case Western Reserve University, Cleveland, OH 44106, USA; [3]University Hospitals Cleveland Medical Center, Cleveland, OH 44106, USA; [4]Molecular Theranostics, Cleveland, OH 44114, USA. *Equal contributors.*

Abstract: Patients diagnosed with pancreatic cancer at a late stage have a dismal survival rate. Accurate early detection of pancreatic cancer with a size of 10 mm or less could dramatically improve patient survival after timely treatments. We have developed a new PET probe ZD2-(68Ga-NOTA) specific to extradomain-B fibronectin (EDB-FN), an oncoprotein in tumor microenvironment, for sensitive molecular imaging and early diagnosis of pancreatic cancer. A targeted ligand ZD2-NOTA is synthesized by conjugation of a macrocyclic ligand NOTA via a 6-aminohexanoic acid spacer to a linear ZD2 peptide (Thr-Val-Arg-Thr-Ser-Ala-Asp). ZD2-(68Ga-NOTA) is synthesized by relabeling of ZD2-NOTA with $^{68}GaCl_3$ in a high purity under GMP conditions. The expression of EDB-FN is demonstrated in BxPC3 and Capan-1 human pancreatic cancer cells and tumor xenografts in mice. ZD2-(68Ga-NOTA) results in significantly higher uptake in the both BxPC3 and Capan-1 tumor xenografts than normal organs and tissues, including the brain, heart, liver and muscle, at 1 hr postinjection in mice. The tumor to muscle uptake ratio is at least 5 folds for the tracer in both tumors. ZD2-(68Ga-NOTA) is able to clearly delineate the PaCa tumors with a size of 10 mm or less with minimal background noise in normal tissues, including the liver. Substantial tumor uptake is still visible at 2 hr post-injection. The results suggest that the ZD2 peptide targeted PET probe has a potential for sensitive molecular imaging of EDB-FN and early detection of pancreatic cancer to improve healthcare of the patients diagnosed with the disease.

Keywords: ZD2 peptide, EDB fibronectin, PET, pancreatic cancer, 68Ga-NOTA

Introduction

Early detection and diagnosis of pancreatic cancer (PaCa) is pivotal to improve the survival of PaCa patients. Although PaCa accounts for only 3% of all cancers, it causes about 7% of all cancer deaths, and represents the 3rd leading cause of all cancer deaths. The 5-year survival rate of patients diagnosed with PaCa is mere 9% [1]. The poor prognosis is due to the fact that most of the cases are diagnosed at an advanced stage when the disease has advanced locally or metastasized in other organs, and in both scenarios, and limited treatment options are available for cure. The 5-year survival of the patients diagnosed with advanced PaCa is close to zero as compared to

24% for those diagnosed with localized disease [2, 3]. The 5-year survival rate can be improved to 80-100% if PaCa is detected and treated when the size of the tumor is 10 mm or less [4]. Therefore, accurate early detection and diagnosis of PaCa are critical to improve the survival of the patients [5, 6]. However, the currently available diagnostic tools, including ultrasound, CT, MRI and PET, could not provide accurate detection, diagnosis, staging of PaCa in clinical practice [7]. Development of novel non-invasive diagnostic imaging approaches is critical to address this unmet clinical need to improve the healthcare of patients with PaCa.

Molecular imaging with PET has the potential to improve the diagnosis of PaCa once a suitable

onco-protein is identified and a specific tracer to the molecular target is developed [8]. Extradomain B fibronectin (EDB-FN) is a promising molecular target for designing PET tracers for the diagnosis of PaCa. It is an oncofetal isoform of fibronectin abundant in the extracellular matrix (ECM) and perivascular space in various aggressive cancers but absent in normal tissues [9, 10]. EDB-FN is a marker of epithelial-to-mesenchymal transition (EMT), a process associated with drug resistance and metastatic invasion in aggressive cancers [11-14]. Strong expression of EDB-FN in the primary tumors is correlated with a high incidence of metastasis and poor overall survival of patients diagnosed with pancreatic, prostate, breast, ovarian, and head and neck cancer [13, 15, 16]. Specifically, for PaCa, EDB-FN is found overexpressed in the tumor, with no expression in normal pancreatic tissue or pancreatitis [10]. The presence of EDB-FN in PaCa tumor ECM will allow rapid and specific binding of a targeted tracer for sensitive molecular imaging and PaCa diagnosis.

We have recently identified a peptide ZD2 (Thr-Val-Arg-Thr-Ser-Ala-Asp) with specific binding to EDB-FN [17]. ZD2 peptide has been used in the development of targeted MRI contrast agents for cancer imaging [18, 19]. ZD2 targeted MRI contrast agents have exhibited the capacity for detecting aggressive solid tumors, including prostate cancer and breast cancer, and differentiating aggressive tumors from less invasive tumors. Herein, we synthesized a ZD2 peptide targeted ^{68}Ga-NOTA conjugate, ZD2-(^{68}Ga-NOTA), as a PET probe for sensitive molecular imaging of EDB-FN and accurate detection of pancreatic cancer. Gallium-68 (^{68}Ga) is a positron emitter with a reasonable half-life ($t_{1/2}$=67.7 min) and has been used for developing cancer specific PET tracers [20]. The targeted ligand ZD2-NOTA was synthesized by conjugating ZD2 peptide to NOTA via 6-aminohexanoic acid. High expression of EDB-FN was shown in PaCa tumor tissues from mice bearing human PaCa tumor xenografts. The effectiveness of ZD2-(^{68}Ga-NOTA) for PET imaging was shown in two mouse tumor models of human PaCa.

Results

Chemical synthesis

The peptide targeted PET tracer ZD2-(^{68}Ga-NOTA) was synthesized according to the proce-

dures depicted in **Figure 1**. Macrocyclic ligand NOTA was used because it could readily form stable chelate with ^{68}Ga (III) under relatively mild conditions for a short reaction time, which is critical for achieving relatively high yield of radiochemical labeling. 6-Aminohexanoic acid (HA) was used as a spacer for conjugation of NOTA to the peptide. Both the precursor ligand and cold chelate were synthesized in high yield and purity. **Figure 2** shows the MALDI-TOF mass spectra and HPLC chromatograms of ZD2-NOTA and ZD2-(Ga-NOTA). The HPLC purity of the targeted ligand was approximately 98% after purification with preparative HPLC. ZD2-(Ga-NOTA) had an excellent water-solubility, which is an advantageous feature for minimizing non-specific tissue binding. The radioactive tracer ZD2-(^{68}Ga-NOTA) was synthesized by reacting ZD2-NOTA with ^{68}GaCl$_3$ in a high yield and high purity as well as with low endotoxin contamination under the standard GMP conditions for ^{68}Ga tracers.

Expression of EDB-FN in human pancreatic cancer cells and tumor xenografts

The expression of EDB-FN in BxPC3 and Capan-1 human pancreatic cancer cell lines was determined with RT-PCR and Western blotting. Although BxPC3 cells had much higher EDB-FN expression than Capan-1 at the mRNA levels, the expression of EDB-FN at the protein level was comparable in both cell lines, **Figure 3A**, **3B**. The haemotoxylin and eosin (H&E) staining of histological sections of human BxPC3 and Capan-1 human pancreatic tumor xenografts showed that both tumors were poorly differentiated carcinoma, i.e., high grade tumors (**Figure 3C**). EDB-FN expression was also determined in the tumor sections using immunofluorescence staining with BC-1 anti-EDB-FN monoclonal antibody [21]. As shown in **Figure 3D**, substantial expression of EDB-FN was observed in both BxPC3 and Capan-1 tumors, with no expression in normal pancreas and muscle, consistent with the reported results [10]. The expression of EDB-FN was mainly observed in the extracellular matrix of the PaCa tumors. The results indicate that EDB-FN is highly expressed by PaCa cells and tumors.

ZD2 peptide binding to EDB-FN in PaCa tumors

Specific binding of ZD2 peptide to EDB-FN in pancreatic tumors was tested by incubating
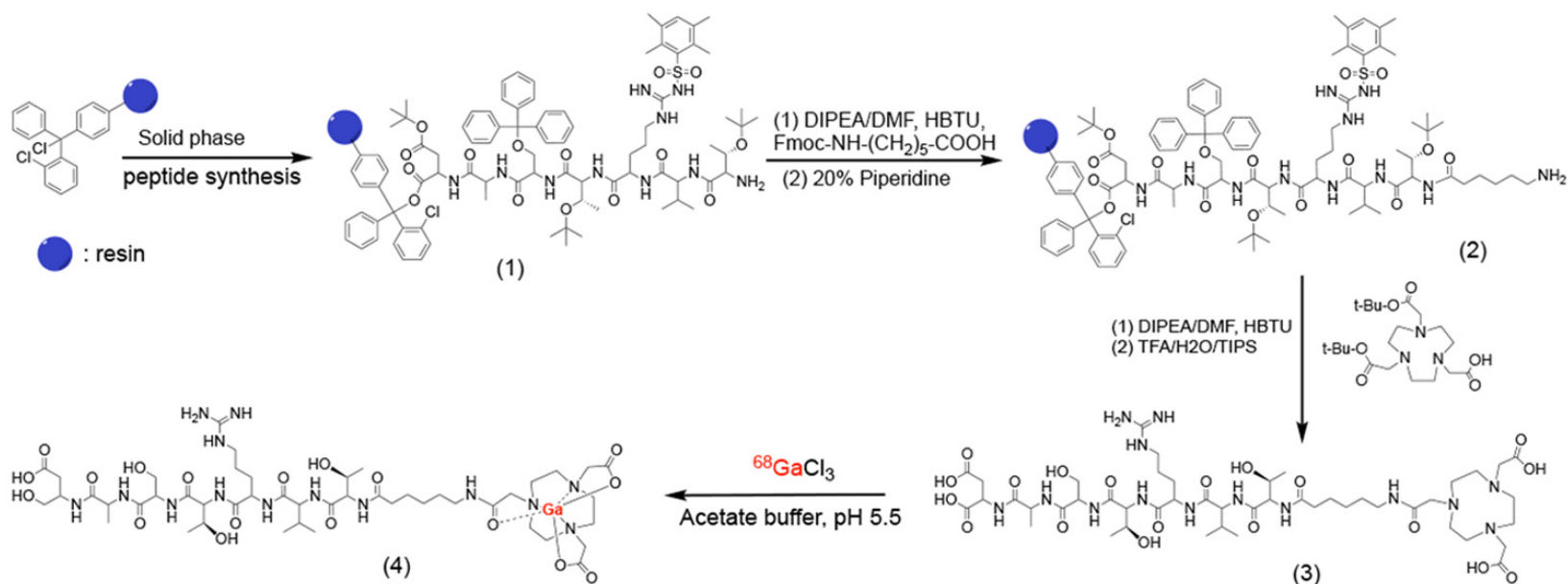
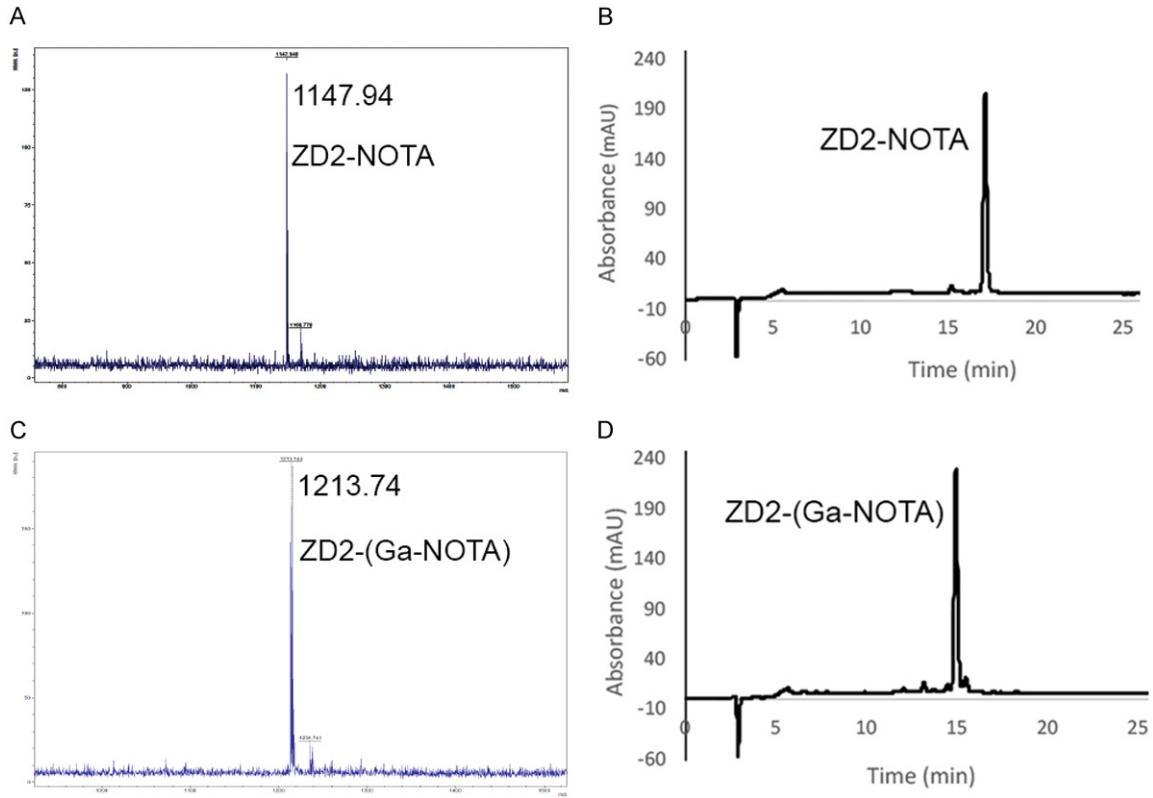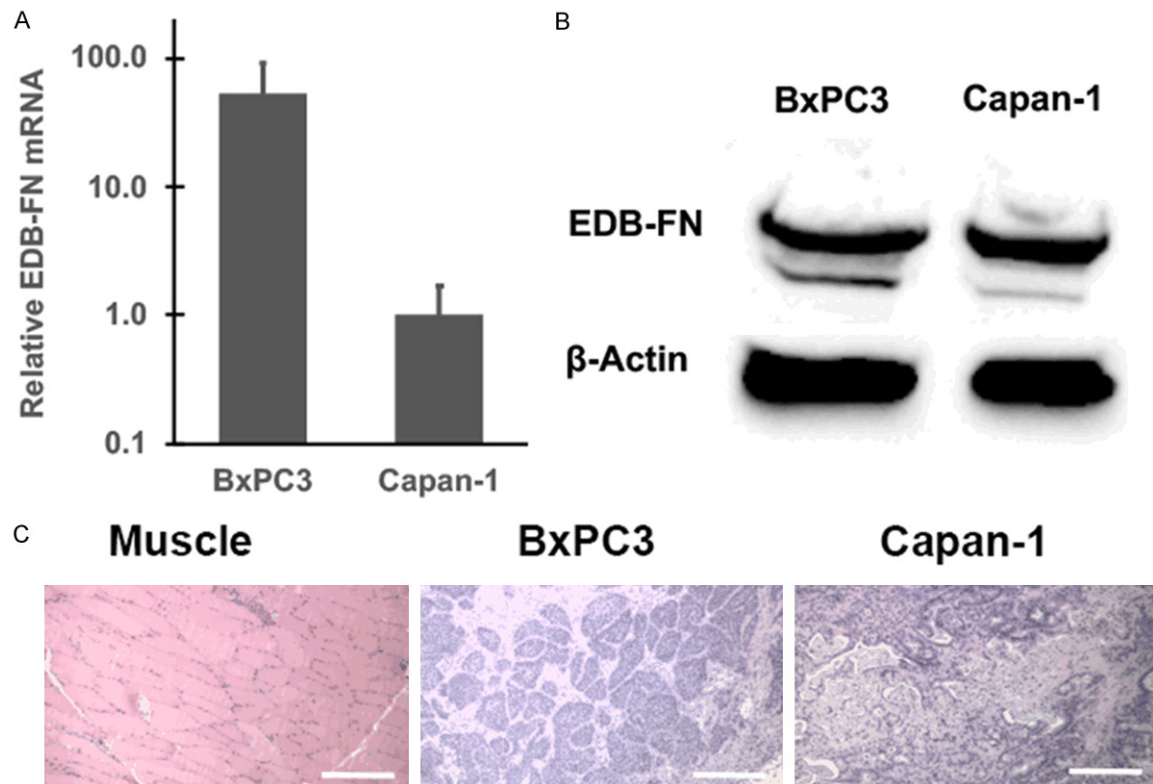**Figure 1.** The synthesis procedure of ZD2-(^{68}Ga-NOTA) (4).

Figure 2. MALDI-TOF mass spectra and HPLC chromatograms of ZD2-NOTA (A, B) and cold ZD2-(Ga-NOTA) (C, D).
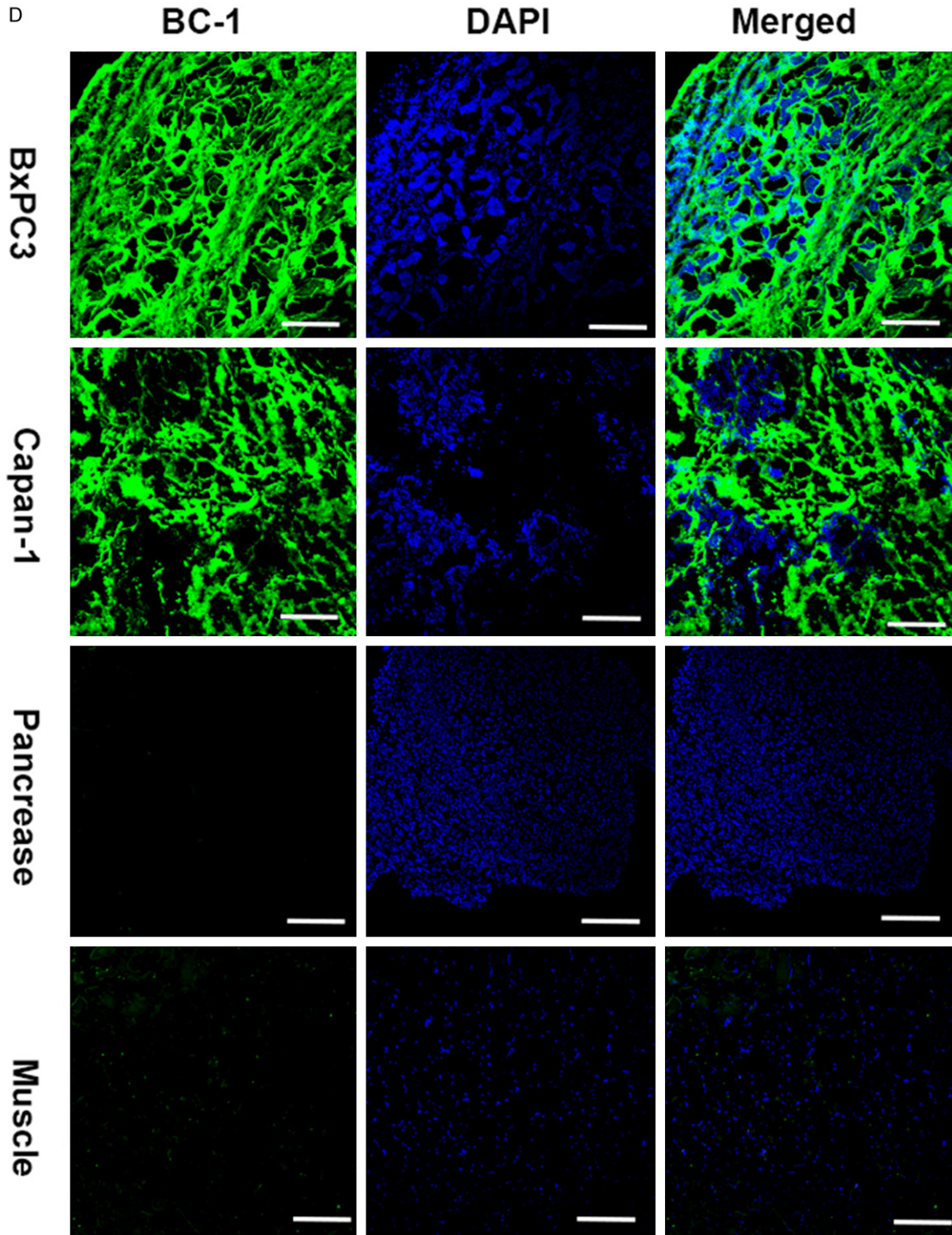
Figure 3. RT-PCR (A), Western blots (B), showing the expression of EDB-FN in BXPC3 and Capan-1 human pancreatic cancer cells (A, B), and haemotoxylin and eosin (H&E) histological images (C) and immunofluorescence staining of the tumor xenografts from the tumor bearing mice (D). The tissue slides were stained with BC-1 anti-EDB-FN monoclonal antibody and a secondary antibody labeled with AF-488 (green) and DAPI (blue) (D). Scale bar: 200 μm.

ZD2-Cy5.5 with the BxPC3 and Capan-1 tumor sections. As shown in **Figure 4**, strong binding of ZD2-Cy5.5 (red) was observed in both PaCa tumor tissues, similar to the immunofluorescence staining in **Figure 3**. No significant binding of ZD2-Cy5.5 was observed to the normal
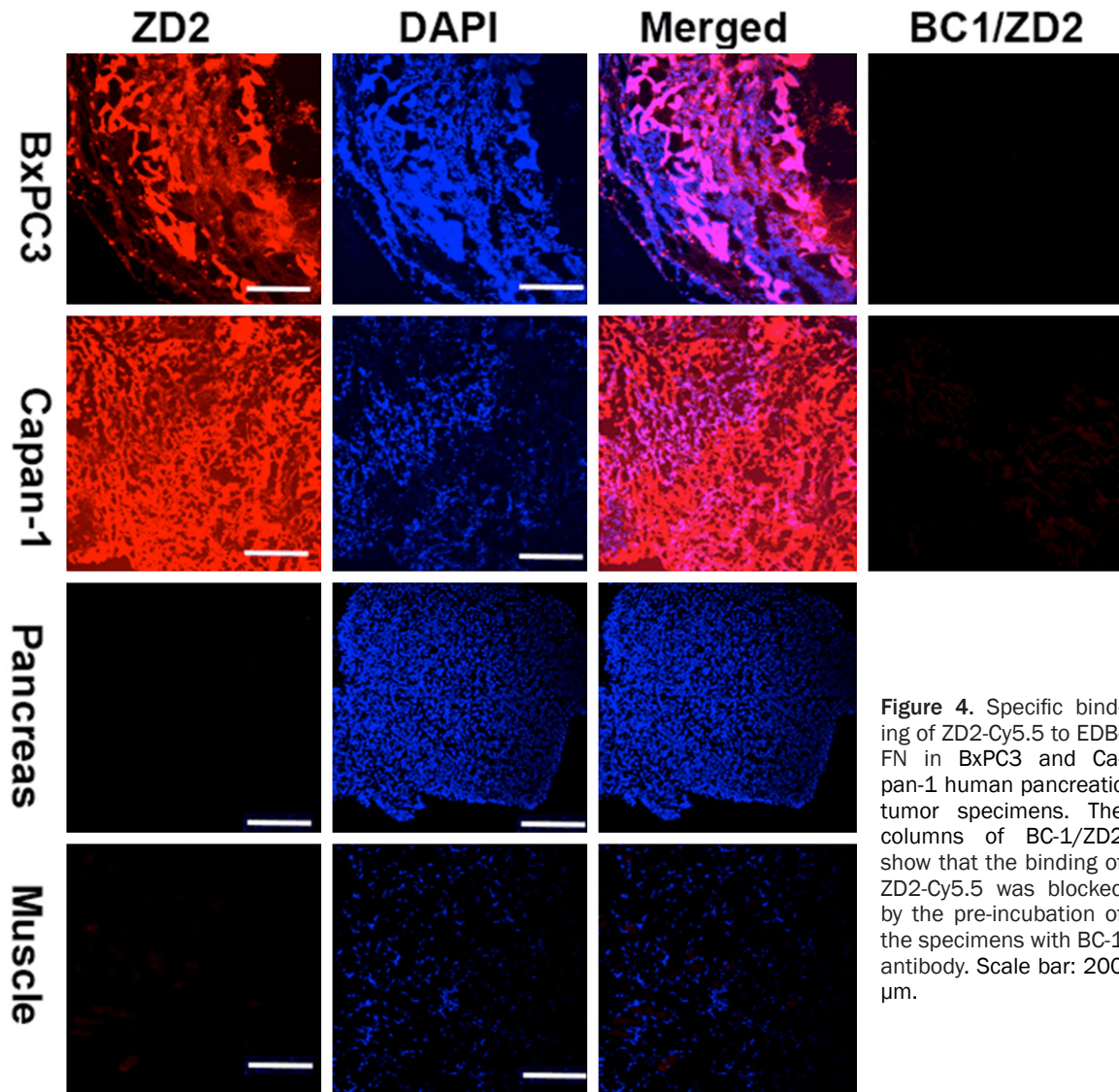
Figure 4. Specific binding of ZD2-Cy5.5 to EDB-FN in BxPC3 and Capan-1 human pancreatic tumor specimens. The columns of BC-1/ZD2 show that the binding of ZD2-Cy5.5 was blocked by the pre-incubation of the specimens with BC-1 antibody. Scale bar: 200 μm.

pancreas and muscle. Little fluorescence staining with ZD2-Cy5.5 was observed for the PaCa specimens pre-incubated with BC-1 antibody, indicating blockage of ZD2-Cy5.5 binding by BC-1 antibody (BC-1/ZD2). The results suggest that both ZD2-Cy5.5 and BC-1 specifically bind to the same EDB-FN protein target in the tumor tissues. No binding of ZD2-Cy5.5 was observed in the normal pancreas and muscle tissues. Taken together, ZD2 peptide is a promising targeting agent for specific binding of EDB-FN in PaCa tumors.

PET imaging of PaCa with ZD2-(^{68}Ga-NOTA)

The effectiveness of ZD2-(^{68}Ga-NOTA) for sensitive molecular imaging of EDB-FN and detec-

tion of PaCa was assessed in the mouse models bearing Capan-1 and BxPC3 human PaCa xenografts on a microPET/CT. **Figure 5** shows the representative 2D axial and coronal as well as 3D whole body PET/CT images of the tumor bearing mice at 1 and 2 hr postinjection. Strong uptake of the tracer was observed in the tumors, kidneys and bladder at 1 hr post-injection as shown in the whole-body PET images. The uptake of the tracer in both tumors was substantially higher than the normal organs and tissues, including the brain, heart, liver, and muscle. High signal intensity in the kidneys and bladder indicates that the tracer is mainly excreted via renal filtration. Significant radioactivity was still visible for delineation of the tumor tissues at 2 hr post-injection.
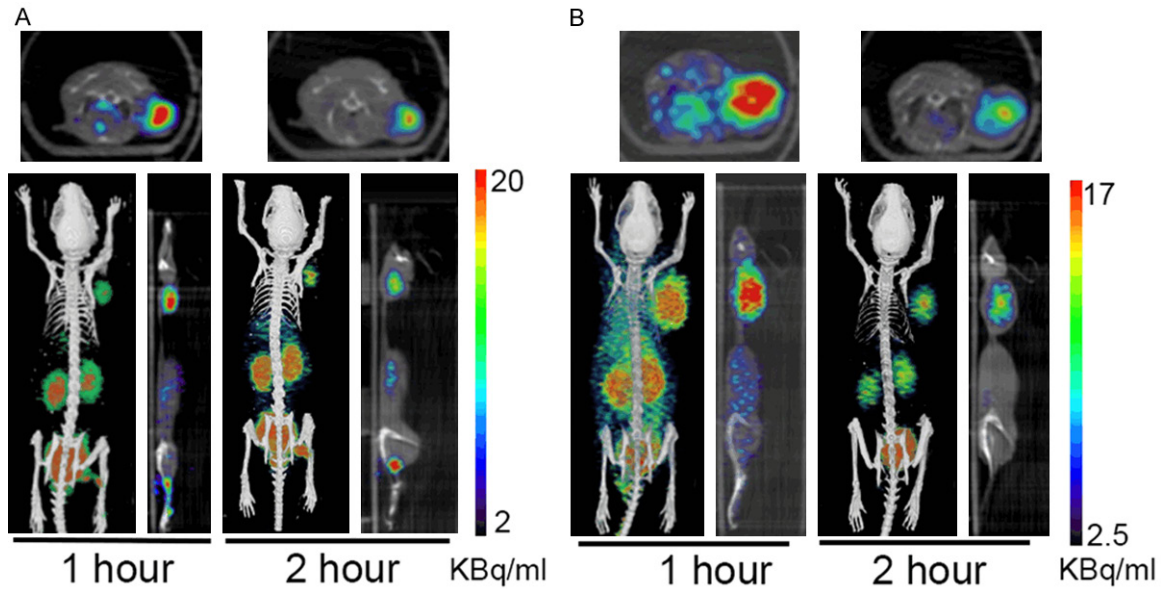
Figure 5. Two-dimensional and three-dimensional PET/CT images of mice bearing BxPC3 (A) and Capan-1 (B) human pancreatic cancer xenografts at 1 and 2 hr after intravenous injection of ZD2-(^{68}Ga-NOTA). B: bladder; K: kidneys; T: tumor.

Quantitative analysis revealed that the uptake in both tumors was significantly higher than the normal tissues, including brain, heart, liver and muscle, at 1 hr post-injection, **Figure 6**. The tumor uptake of ZD2-(^{68}Ga-NOTA) was approximately 5.4 and 5.6 fold of that of the muscle (P<0.01), 10 and 11 fold of the brain (P<0.01), 1.6 and 2.2 fold of the liver (P<0.05), and 2.4 and 2.0 fold of the heart (P<0.05) for BxPC3 and Capan-1 tumors, respectively, at 1 hr post-injection. The tumor uptake remained significantly higher than the normal tissues in both tumor models (P<0.05) except for the liver of BxPC3 tumors at 2 hr post-injection. These results demonstrate that ZD2-(^{68}Ga-NOTA) is highly specific to PaCa tumors with minimal uptake in normal tissues, including the liver.

Biodistribution

The biodistribution of ZD2-(^{68}Ga-NOTA) in different organs and tissues was determined at 3 hr post-injection. **Figure 7** shows the uptake of the imaging agent in the tumor, brain, heart, kidneys, large intestine, liver, lungs, muscle, small intestine, stomach, and spleen in both tumor models measured with a γ-counter. Consistent to the uptake obtained from the PET images, the uptake in both tumors was significantly higher than the tested organs (P<0.05) except for the liver, small intestine and kidney. As com-

pared to the data in **Figure 6**, the increased uptake in the liver at 3 hr post-injection could be attributed to the increased excretion of the tracer by the liver, which is supported by the increased uptake in the small intestine. The uptake of ZD2-(^{68}Ga-NOTA) in the BxPC3 and Capan-1 tumors was approximately 4.4 and 5.0 fold of that of the muscle (P<0.05), respectively, 14 fold of the brain (P<0.01), 3 fold of the heart (P<0.05). The biodistribution data validated the observations of specific uptake of ZD2-(^{68}Ga-NOTA) in the PaCa tumors observed with PET imaging.

Discussion

Currently, diagnostic imaging, blood tests and histopathology following tissue biopsy are the commonly used diagnostic tools for the detection and diagnosis of PaCa [8, 22-26]. The standard clinical imaging for PaCa diagnosis can be improved by using PET imaging, especially for small lesions, once an effective PET tracer is available. Despite substantial efforts in developing non-invasive imaging agents, no probe is yet available for effective molecular imaging and clinical management of PaCa. The main challenges remain to be the identification of imageable molecular targets specific to PaCa and the dense tumor stroma of PaCa that limits the access to the markers expressed on cancer
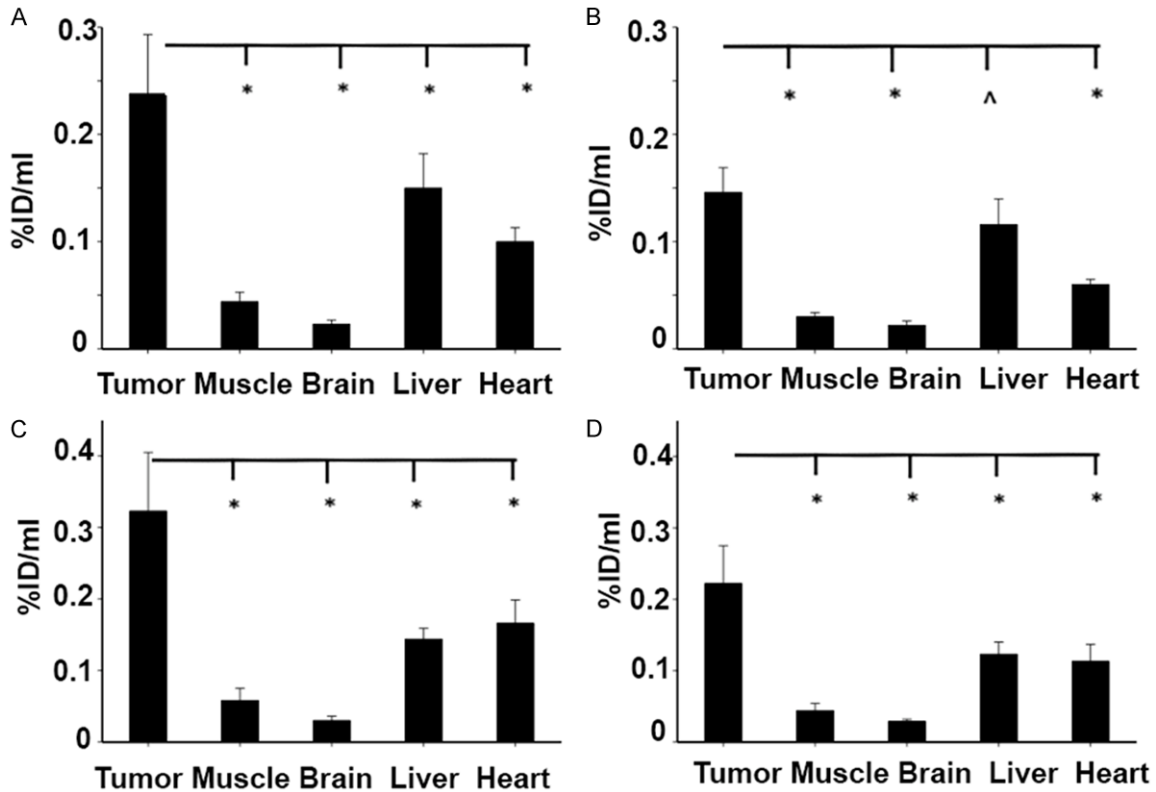
Figure 6. The uptake of ZD2-(^{68}Ga-NOTA) in the BxPC3 (A, B) and Capan-1 (C, D) human PaCa tumor xenografts determined from the PET images in comparison with those in the muscle, brain, liver, and heart at 1 (A, C) and 2 (B, D) hr post-injection (n=5, *P<0.05; $^\wedge$P>0.05).
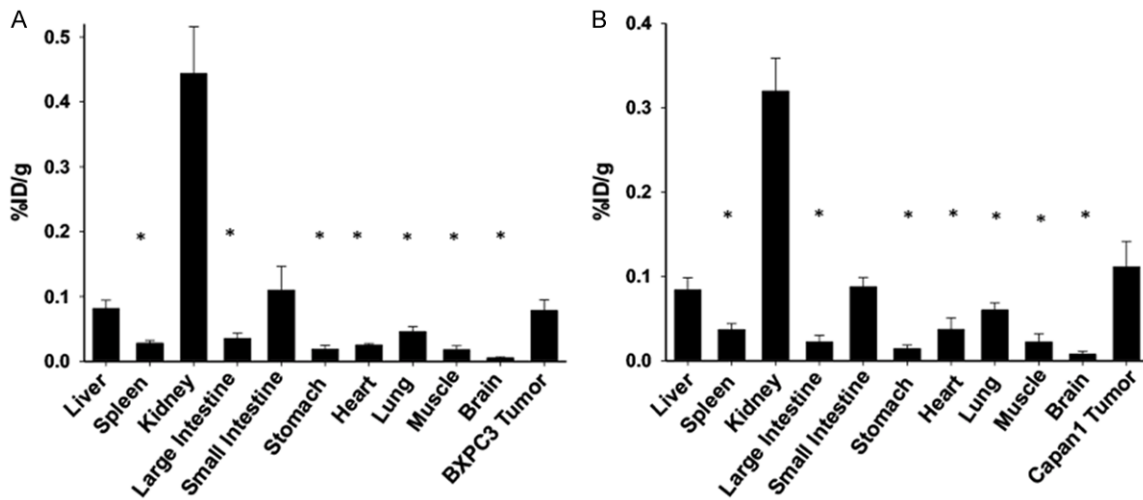
Figure 7. The biodistribution of ZD2-(^{68}Ga-NOTA) in the BxPC3 (A) and Capan-1 (B) human PaCa tumor xenografts, brain, heart, kidneys, large intestine, liver, lungs, muscle, small intestine, spleen, and stomach determined at 3 post-injection with a gamma counter. (n=5, *P<0.05 when the organ or tissue is compared to the tumor).

cell surface. In this study, we have explored EDB-FN as an oncoprotein potential for sensitive molecular imaging of PaCa with PET.

Fibronectin, including EDB-FN, is previously known as a marker for tumor angiogenesis [15]. It has been recently found to be associat-

ed with EMT of many types of aggressive human cancers and is highly expressed in tumor ECM to facilitate cancer invasion and drug resistance [11, 17, 27, 28]. It exhibits several advantageous features to serve as a molecular target for PaCa imaging. Highly specific expression of EDB-FN in tumor ECM allows facile access and efficient binding of the tracer for imaging and delineation of PaCa. Because most aggressive tumors have similar unique ECM compositions, molecular imaging of the ECM oncoprotein has the potential to overcome the limitations of molecular imaging of the biomarkers expressed on cancer cell surface, including poor access for target binding, and heterogeneous and inconsistent expression of biomarkers on cancer cell surface.

The expression of EDB-FN in BxPC3 and Capan-1 human PaCa cells and tumor xenografts is verified using different assays. It appears that BxPC3 cells have much higher EDB-FN expression than Capan-1 cells in culture at the mRNA level, **Figure 3**. However, EDB-FN expression is comparable at the protein level. Histological assessment of the tumor xenografts has confirmed that both PaCa tumor models are high grade tumors. Both tumors have comparable high expression of EDB-FN in tumor ECM as shown by immunofluorescence staining with BC-1 monoclonal antibody (**Figure 3D**). Specific binding of ZD2 peptide is shown in the PaCa tumor specimens with little non-specific binding to normal tissues (**Figure 4**), consistent to the immunofluorescence staining. Consequently, ZD2-(^{68}Ga-NOTA) has a strong tumor uptake with minimal non-specific binding in the normal tissues at 1 and 2 hr post-injection, **Figure 5**.

Quantitative analysis has revealed that ZD2-(^{68}Ga-NOTA) results in approximately 5 fold uptake in both BxPC3 and Canpan-1 tumors as compared to the surrounding muscle tissues. The binding affinity of the linear ZD2 peptide to the EDB fragment is approximately 2 μM as previously reported [18]. Despite of the relatively low binding affinity of the peptide, abundant expression of EDB-FN in the tumor ECM facilitates specific binding and high tumor uptake of the tracer. As shown in **Figure 5**, the unbound tracer is mainly excreted via renal filtration into the bladder. Relatively high non-specific uptake of the tracer is observed in the liver as compared to other normal organs and tissues, indi-

cating that a small fraction of the tracer is excreted via the liver, which is one of excretory organs. Nevertheless, the non-specific liver uptake of ZD2-(^{68}Ga-NOTA) is much lower than the previously reported ZD2-(^{64}Cu-DOTA), which has high liver uptake due to the poor chelation stability of ^{64}Cu-DOTA monoamide chelate and release of the ^{64}Cu [29]. In contrast, ^{68}Ga-NOTA has a much higher chelation stability than ^{64}Cu-DOTA monoamide. Consequently, specific tumor uptake of ZD2-(^{68}Ga-NOTA) is significantly higher than non-specific uptake in the liver. The specific tumor uptake of ZD2-(^{68}Ga-NOTA) is sufficient for detection and delineation of the PaCa tumors in the animal models. The tumor size used in this study is 10 mm in diameter or less. ZD2-(^{68}Ga-NOTA) is effective to detect both PaCa tumors in the mouse models with micro-PET/CT. The results suggest that the tracer has the potential to detect PaCa tumors with size less than 1 cm, which is a critical detection threshold for timely therapeutic interventions for achieving long-term survival of PaCa patients.

Monoclonal antibodies have been developed for specific targeting of EDB-FN in cancer. PET probes have been developed and tested using some of the antibodies or their fragments. Because of their large size and long circulation, a long waiting time is needed for the clearance of the unbound tracer from the circulation and background before specific cancer imaging [30], which is not convenient for both the patients and clinicians. ZD2-(^{68}Ga-NOTA) is a small molecular PET probe constituted with a seven-amino acid peptide and a ^{68}Ga-NOTA chelate. It can be readily synthesized with the existing GMP facility for clinical Ga-68 tracers in a high yield and purity. Both the peptide and ZD2-(^{68}Ga-NOTA) are hydrophilic and highly water-soluble. The small size of ZD2-(^{68}Ga-NOTA) allows facile diffusion into the tumor tissues for effective binding to EDB-FN in the tumor ECM. Its high hydrophilicity would also minimize non-specific interactions with normal tissues, especially in the liver, and allow rapid clearance of the unbound tracer from the background and circulation via renal filtration for timely and effective diagnostic imaging, as shown in **Figure 5**.

Further optimization and assessment of the ZD2 targeted Ga-68 tracer are needed before

clinical development for PaCa imaging. ZD2-(⁶⁸Ga-NOTA) is currently prepared at 125°C and the high temperature may cause degradation of the peptide, which could reduce binding specificity of the tracer. The stability of the peptide at different temperatures needs to be determined to identify an optimal mild radiochemical labeling condition to minimize possible degradation of the peptide. An alternative chelating ligand that forms stable chelate with Ga-68 under mild condition could be used to develop an optimized ZD2 targeted ligand [31]. Although the PET tracers are generally administered at micro doses, comprehensive preclinical assessments of the ZD2 targeted Ga-68 tracer, including safety and biodistribution, are still needed to satisfy the requirements from the regulatory agencies before clinical assessment.

Sensitive and quantitative molecular imaging of EDB-FN with the ZD2 peptide targeted PET probe has the potential to be used for precise and accurate detection and localization of PaCa in clinical practice. ZD2-(⁶⁸Ga-NOTA) can be used for early diagnosis of PaCa in high-risk patient populations, and detection and delineation PaCa tumors in the patients suspicious of the disease after the initial liquid biopsy screening. The tracer can also be used for planning surgery and multimodality treatment as well as monitoring treatment outcomes. Clinical evidence has shown that EDB-FN is highly expressed in many types of aggressive human cancers, including breast, head and neck, and prostate cancers. In previous studies, we have shown that ZD2 targeted MRI contrast agents are effective for detection and risk-stratification of other types of aggressive solid tumors, including breast and prostate cancers, in animal models [18, 19]. Therefore, the ZD2 targeted PET probe has the potential for sensitive and accurate molecular imaging of a broad spectrum of aggressive solid tumors beside pancreatic cancer. ZD2 targeted ligands can also be used for tumor specific delivery of therapeutic nuclides for radiation therapy of cancer after diagnostic imaging with PET tracer.

In summary, ZD2-(⁶⁸Ga-NOTA) was synthesized as a PET probe specific to EDB-FN for molecular imaging and early detection of pancreatic cancer. Specific expression of EDB-FN was shown in two commonly used BxPC3 and Capan-1 human PaCa cells and tumor tissues. ZD2 peptide specifically binds to EBD-FN expressed in the PaCa tumor tissues. ZD2-(⁶⁸Ga-NOTA) has shown specific tumor uptake in the PaCa tumors with minimal uptake in normal tissues, including the liver, at 1 hr postinjection. ZD2-(⁶⁸Ga-NOTA) was effective for detecting small PaCa tumors with a size of 10 mm or less with PET. The peptide targeted PET tracer specific to EDB-FN has the promise for accurate early detection of pancreatic cancer.

Materials and methods

Materials

Protected amino acids for peptide synthesis were purchased from Novabiochem (Burlington, MA). N,N-Diisopropylethylamine (DIPEA) was bought from MP Biomedical LLC (Santa Ana, CA). O-Benzotriazole-N,N,N',N'-tetramethyl-uronium-hexafluorophosphate (HBTU) was purchased from Anaspec Inc (Fremont, CA). Fmoc-6-aminohexanoic acid was purchased from Chem-IMPEX International (WD, IL). t-Butyl bromoacetate was bought from Sigma-Aldrich (St. Louis, MO). All other chemical reagents were purchased from ThermoFisher (Waltham, MA). Bis(*tert*-butyl)-1,4,7-triazacyclononane-1,4,7-triacetate [NOTA-bis(t-Bu ester)] was synthesized according to a reported method [18]. An anti-EDB-FN monoclonal antibody BC1 was purchased from Abcam (Cambridge, MA). A ZD2 peptide targeted fluorescence tracer ZD2-Cy5.5 was synthesized according to a reported method to assess the binding of the peptide to EDB-FN in PaCa tumors [17]. ¹H-NMR spectra were acquired on a 500 MHz Varian Inova NMR spectrometer (Palo Alto, CA) using TMS as an internal standard. Matrix-assisted laser desorption/ionization time-of-flight (MALDI-TOF) mass spectra were obtained on a Voyager DE-STR spectrometer (PerkinElmer, Waltham, MA) in linear mode with 2, 5-dihydroxybenzoic acid as a matrix.

Synthesis of ZD2-NOTA

ZD2 peptide was first synthesized using standard solid phase chemistry as previously reported [18]. 6-Aminohexanoic acid (HA) was then conjugated to N-terminus of the peptide on the resin. A mixture of 6-Fmoc-aminohexanoic acid (1.5 eq.), HBTU (1.5 eq.), DIPEA (1.5

eq.) in 10 mL anhydrous DMF was added to the resin at the end of peptide synthesis (0.5 mmol peptide) and was shaken until all amino groups are conjugated based on Kaiser test. The resin was then washed with DMF (10 mL × 3) and dichloromethane (10 mL × 3). Small amount of the resin beads was treated with a cocktail of TFA:H_2O:TIBS (96.5:2.5:1) for 30 minutes to verify ZD2-HA structure with MALDI-TOF mass spectrometry [m/z (M+1): 862.47, observed; 861.45, calculated]. The resin was finally mixed with NOTA-bis (t-Bu ester) (0.312 g, 0.75 mmol), HBTU (0.284 g, 0.75 mmol), DIPEA (0.097 g, 0.75 mmol) in 10 mL anhydrous DMF and was shaken until all amino groups are conjugated. The resin then was washed using DMF (10 mL × 3) and DCM (10 mL × 3). ZD2-HA-NOTA was subsequently cleaved from the resin for 3 hours using a cocktail of TFA:H_2O:TIBS (96.5:2.5:1) and was precipitated in cold ethyl ether. The product was purified using Agilent 1100 HPLC with a preparative ZORBAX 300 SB-C18 column (Santa Clara, CA) with the following conditions: eluent A, H_2O/TFA (0.1%); B, MeCN/TFA (0.1%); 0% B for 15 min, 0-50% B for 30 min, 50% B for 5 min, 50%-100% B for 2 min, 100% B for 5 min, flow rate 2 mL/min, UV-detection at 210 nm. The final product was characterized by MALDI-TOF mass spectrometry (m/z [M+1]: 1147.56, observed; 1147.25, calculated for $C_{47}H_{83}N_{15}O_{18}$).

Synthesis of ZD2-(Ga-NOTA)

To the solution of ZD2-NOTA (0.11 g, 0.1 mmol) in 10 mL of NaAc-Ac buffer solution (0.1 M, pH 5.5) and Ga(NO$_3$)$_3$ (0.076 g, 0.3 mmol) was added. The solution was stirred for overnight at room temperature, and the product was purified using preparative HPLC and lyophilized to give a white powder. Yield: 43%. The product was characterized by MALDI-TOF mass spectrometry (m/z [M+1]: 1213.54, observed; 1213.51; calculated for $C_{47}H_{82}GaN_{15}O_{18}$).

Synthesis of radiolabeled ZD2-(^{68}Ga-NOTA)

The radiosynthesis was performed in closed-system fully automated Scintomics GRP® synthesizer (Furstenfeldbruck, Germany). ^{68}Ge/^{68}Ga generator (model IGG-100) was purchased from Eckert & Ziegler Isotope Products (Berlin, Germany). In the process of automated synthesis, ^{68}Ga (III) was eluted from ^{68}Ge/^{68}Ga generator with 0.1 M hydrochloric acid, and the eluent

was diluted with water. The resulting solution was passed through the cationic exchange PS-H$^+$ cartridge and subsequently eluted with 5 M sodium chloride solution into the pre-heated reactor containing ZD2-NOTA and HEPES buffer. The labeling was performed in 10 minutes at 125°C. After reaction, the reaction content was transferred onto C18 Plus Light SPE-cartridge, and the labeled ZD2-(^{68}Ga-NOTA) was eluted with a mixture of water for injection/ethanol (1/1, v/v) through the 0.22 μm membrane sterile filter into the final product vial. Finally, the product was diluted with PBS buffer through the same sterile 0.22 μm membrane filter into the final product vial. Samples are then aseptically removed for quality control testing. The typical d.c. RCY is ~71% (~54% n.d.c. RCY at EOS). Quality control tests similar to those for clinical formulations of [^{68}Ga] Ga-labeled peptides showed that product solution was colorless without particles, pH=7.0, endotoxin test <2 EU/mL, radiochemical purity >90% as show by HPLC (C18 RP column, 0.1% TFA/H_2O-0.1% TFA/ACN).

Cell culture and animal tumor models

Capan-1 and BxPC3 human PaCa cancer cells (ATCC, Manassass, VA) were cultured in a tissue culture incubator (Thermo Scientific, Waltham, MA) in 5% CO_2 and 37°C. The cells were grown in DMEM media (Gibco, Waltham, MA) with 10% fetal bovine serum (Gibco, Waltham, MA), and 1% Penicillin Streptomycin (Gibco, Waltham, MA). The animal models of PaCa were developed by subcutaneous implant of Capan-1 and BxPC3 human pancreatic cancer cells in female athymic nu/nu mice (8 weeks old). Female athymic nude mice were purchased from the Case Comprehensive Cancer Center (Cleveland, OH, USA) and cared for in the Animal Core Facility of Case Western Reserve University. All experiments were conducted in accordance to an animal protocol approved by the CWRU Institutional Animal Care and Use Committee. The mice were anesthetized with isoflurane delivered through a veterinary vaporizer at a concentration of 2.5% with 2.5 lpm O_2, and subcutaneously implanted with the cancer cell (8 × 10^6) in Matrigel (100 μL) in the superior flank of each mouse. Tumor size was monitored bi-weekly with calipers and imaging was performed when size of tumors reached 6-10 mm in diameter.

EDB-FN expression in human PaCa cells

Human PaCa Capan-1 and BxPC3 cells (1 × 10^6, ATCC, Manassas, VA) were plated in a six well plate (Corning, Corning, NY) and allowed to grow for 24 hr. RNA was extracted with the RNeasy Plus kit (Qiagen, Germantown, MD) and measured with UV Spectroscopy. cDNA was generated with the MiScript II RT Kit (Qiagen, Germantown, MD). qPCR was performed on a CFX Connect thermocycler with SYBR Green Master Mix (Applied Biosystems, Foster City, CA) and EDB-FN (Fwd: 5' CCGCTAAACTCTTC-CACCATTA 3' Rev: 5' AGCCCTGTGACTGTGTAGTA 3') and Beta-Actin (Fwd: 5' CATCCACGAAAC-TACCCTTCAACTCC 3' Rev: 5' GAGCCGCCGAT-CCACACG 3') primers with an annealing temperature of 55°C. Data was analyzed with the DDCq method. For Western blotting, the cells were then washed with Dulbecco's Phosphate Buffered Saline (Thermo Fisher, Waltham, MA) and lysed with ice-cold RIPA Buffer (150 mM NaCl, 1.0% Triton X-100, 0.5% Sodium De-oxycholate, 0.1% SDS, 50 mM Tris, pH 8.0). Protein concentration was assayed with the Pierce BCA Protein Assay Kit (Thermo Fisher, Waltham, MA). SDS-PAGE was performed in a 4-20% Acrylamide gel (BioRad, Hercules, CA). Transfer was performed onto PVDF for 3 hours at 70 V in buffer containing 5% (v/v) MeOH. Primary antibody detection for EDB-FN (BC1, Abcam, Cambridge, MA) and Beta-Actin (13E5, Cell Signaling Technologies, Danvers, MA) at a concentration of 1:500 and 1:1000, respectively.

Histological analysis of PaCa tumors

After the mice were euthanized, the tumors were after the mice were collected, embedded in Optimal Cutting Temperature Medium (OCT), frozen in -80°C, cryosectioned at 5 µm and permeabilized with cold acetone. Some of the tissue sections were processed with standard H&E staining. The tissue sections were blocked with bovine serum albumin (1%) in PBS at room temperature for 1 hr and incubated with BC1 antibody for 1 hr. After extensive washing, secondary anti-mouse Alexa Fluor 488 secondary antibody was incubated for 1 hr. Tissue sections were counterstained with Prolong Gold antifade mounting medium with DAPI (Thermo Fisher, Waltham, MA). The stained tissues were imaged on an Olympus FV1000 confocal laser scanning microscope.

ZD2 peptide binding to PaCa tumors

The histological sections of Capan-1 and Bx-PC3 human PaCa xenografts were deparaffinized in xylene, ethanol, and tap water washes, and then blocked with 10% goat serum (Invitrogen, Carlsbad, CA) in PBS with 0.1% Tween 20 (PBS-T) (Gibco, Waltham, MA) for 30 minutes. The tissue slides were incubated with ZD2-Cy5.5 (500 nM) in PBS-T for 1 hour. Following three washes with PBS-T, the sections were mounted using fluoroshield mounting medium with DAPI (Abcam, Cambridge, UK). Images were acquired on a confocal microscope using pre-programmed emission and excitation filters for Cy5.5 (635 nm excitation, 693 nm emission) (Olympus, Tokyo, Japan) and DAPI (405 nm excitation, 461 nm emission). In a competitive experiment, the tissue sections were first incubated with an excess of BC1 antibody for 1 hr, followed by three washes with PBS-T. The sections were then incubated with ZD2-Cy5.5 and analyzed similarly as described above.

PET imaging

All in vivo imaging studies were conducted in accordance with CWRU Animal Research Committee-approved protocols and guidelines. Mice were anesthetized with 2% isoflurane in oxygen. ZD2-(^{68}Ga-NOTA) was injected at a dose of 140-350 µCi [5.3-13.0 MBq] via a tail vein. Then mice underwent 10-min or 20-min static PET scans (Inveon microPET, Siemens Medical Solutions USA Inc.) after 1 hours and 2 hours uptake period. All PET procedures were followed with CT scans for anatomical co-registration. PET/CT images were analyzed using Inveon Research Workplace version 3.0 and AMIRA 6.01 software. Regions of interest (ROIs) were drawn for the tumors and major organs, including brain, heart, kidneys, liver and muscle, to calculate the ratio of specific and non-specific tissue uptake. Images were processed with 3D reconstruction with a zoom factor of 1.0 using 3D-OSEM with two iterations followed by MAP with 18 iterations.

Biodistribution

After the PET imaging, the mice were euthanized at 3 hr post-injection. Major organs and tissues, including the brain, heart, kidneys, large intestine, liver, lungs, muscle, small intes-

tine, spleen, and stomach were collected and weighed. The radioactivity in the organs and tissues was determined in a PerkinElmer B291000 gamma counter (Hopkinton, MA). The percent-injected dose per gram of tissue was calculated using a standard containing 2% of the injected dose.

Data analysis

The uptake of the tracer was calculated as a percentage of ROI tissue radioactivity concentration to the administered dose and presented as %ID/ml. The specific uptake in the tumors was compared with the uptake in muscle and other organs using Student's *t*-test assuming equal variance, and the difference was considered significant if $P<0.05$. Data are represented as mean ± s.e.m.

Acknowledgements

Disclosure of conflict of interest

None.

Address correspondence to: Dr. Zhengrong Lu, Department of Biomedical Engineering, Case Western Reserve University, Wickenden 427, Mail Stop 7207, 10900 Euclid Avenue, Cleveland, OH 44106, USA. Tel: 216-368-0187; Fax: 216-368-4969; E-mail: zxl125@case.edu

References

[1] Siegel RL, Miller KD and Jemal A. Cancer statistics, 2018. CA Cancer J Clin 2018; 68: 7-30.

[2] Deplanque G and Demartines N. Pancreatic cancer: are more chemotherapy and surgery needed? Lancet 2017; 389: 985-986.

[3] Zhang L, Sanagapalli S and Stoita A. Challenges in diagnosis of pancreatic cancer. World J Gastroenterol 2018; 24: 2047-2060.

[4] Tsunoda T, Yamamoto Y, Kimoto M, Imai H, Iwamoto S, Kawasaki S, Kawashima K, Tadaoka Y, Majima T, Onuma E, Iki K, Kubozoe T and Eto T. Staging and treatment for patients with pancreatic cancer. How small is an early pancreatic cancer? J Hepatobiliary Pancreat Surg 1998; 5: 128-132.

[5] Yeh R, Steinman J, Luk L, Kluger MD and Hecht EM. Imaging of pancreatic cancer: what the surgeon wants to know. Clin Imaging 2017; 42: 203-217.

[6] Hanada K, Amano H and Abe T. Early diagnosis of pancreatic cancer: current trends and concerns. Ann Gastroenterol Surg 2017; 1: 44-51.

[7] Dimastromatteo J, Brentnall T and Kelly KA. Imaging in pancreatic disease. Nat Rev Gastroenterol Hepatol 2017; 14: 97-109.

[8] Thomas C. Risk factors, biomarker and imaging techniques used for pancreatic cancer screening. Chin Clin Oncol 2017; 6: 61.

[9] Sauer S, Erba PA, Petrini M, Menrad A, Giovannoni L, Grana C, Hirsch B, Zardi L, Paganelli G, Mariani G, Neri D, Durkop H and Menssen HD. Expression of the oncofetal ED-B-containing fibronectin isoform in hematologic tumors enables ED-B-targeted 131I-L19SIP radioimmunotherapy in Hodgkin lymphoma patients. Blood 2009; 113: 2265-2274.

[10] Wagner K, Schulz P, Scholz A, Wiedenmann B and Menrad A. The targeted immunocytokine L19-IL2 efficiently inhibits the growth of orthotopic pancreatic cancer. Clin Cancer Res 2008; 14: 4951-4960.

[11] Freire-de-Lima L, Gelfenbeyn K, Ding Y, Mandel U, Clausen H, Handa K and Hakomori SI. Involvement of O-glycosylation defining oncofetal fibronectin in epithelial-mesenchymal transition process. Proc Natl Acad Sci U S A 2011; 108: 17690-17695.

[12] Menzin AW, Loret de Mola JR, Bilker WB, Wheeler JE, Rubin SC and Feinberg RF. Identification of oncofetal fibronectin in patients with advanced epithelial ovarian cancer: detection in ascitic fluid and localization to primary sites and metastatic implants. Cancer 1998; 82: 152-158.

[13] Santimaria M, Moscatelli G, Viale GL, Giovannoni L, Neri G, Viti F, Leprini A, Borsi L, Castellani P, Zardi L, Neri D and Riva P. Immunoscintigraphic detection of the ED-B domain of fibronectin, a marker of angiogenesis, in patients with cancer. Clin Cancer Res 2003; 9: 571-579.

[14] Han Z and Lu ZR. Targeting fibronectin for cancer imaging and therapy. J Mater Chem B 2017; 5: 639-654.

[15] Kaspar M, Zardi L and Neri D. Fibronectin as target for tumor therapy. Int J Cancer 2006; 118: 1331-1339.

[16] Mhawech P, Dulguerov P, Assaly M, Ares C and Allal AS. EB-D fibronectin expression in squamous cell carcinoma of the head and neck. Oral Oncol 2005; 41: 82-88.

[17] Han Z, Zhou Z, Shi X, Wang J, Wu X, Sun D, Chen Y, Zhu H, Magi-Galluzzi C and Lu ZR. EDB fibronectin specific peptide for prostate cancer

targeting. Bioconjug Chem 2015; 26: 830-838.

[18] Han Z, Li Y, Roelle S, Zhou Z, Liu Y, Sabatelle R, DeSanto A, Yu X, Zhu H, Magi-Galluzzi C and Lu ZR. Targeted contrast agent specific to an oncoprotein in tumor microenvironment with the potential for detection and risk stratification of prostate cancer with MRI. Bioconjug Chem 2017; 28: 1031-1040.

[19] Han Z, Wu X, Roelle S, Chen C, Schiemann WP and Lu ZR. Targeted gadofullerene for sensitive magnetic resonance imaging and risk-stratification of breast cancer. Nat Commun 2017; 8: 692.

[20] Fendler WP, Eiber M, Beheshti M, Bomanji J, Ceci F, Cho S, Giesel F, Haberkorn U, Hope TA, Kopka K, Krause BJ, Mottaghy FM, Schoder H, Sunderland J, Wan S, Wester HJ, Fanti S and Herrmann K. 68Ga-PSMA PET/CT: Joint EANM and SNMMI procedure guideline for prostate cancer imaging: version 1.0. Eur J Nucl Med Mol Imaging 2017; 44: 1014-1024.

[21] Scarpino S, Stoppacciaro A, Pellegrini C, Marzullo A, Zardi L, Tartaglia F, Viale G and Ruco LP. Expression of EDA/EDB isoforms of fibronectin in papillary carcinoma of the thyroid. J Pathol 1999; 188: 163-167.

[22] Swords DS, Firpo MA, Scaife CL and Mulvihill SJ. Biomarkers in pancreatic adenocarcinoma: current perspectives. Onco Targets Ther 2016; 9: 7459-7467.

[23] Toft J, Hadden WJ, Laurence JM, Lam V, Yuen L, Janssen A and Pleass H. Imaging modalities in the diagnosis of pancreatic adenocarcinoma: a systematic review and meta-analysis of sensitivity, specificity and diagnostic accuracy. Eur J Radiol 2017; 92: 17-23.

[24] Cohen S and Kagen AC. Preoperative evaluation of a pancreas mass: diagnostic options. Surg Clin North Am 2018; 98: 13-23.

[25] Chang JC and Kundranda M. Novel diagnostic and predictive biomarkers in pancreatic adenocarcinoma. Int J Mol Sci 2017; 18.

[26] Lewis AR, Valle JW and McNamara MG. Pancreatic cancer: are "liquid biopsies" ready for prime-time? World J Gastroenterol 2016; 22: 7175-7185.

[27] Javle MM, Gibbs JF, Iwata KK, Pak Y, Rutledge P, Yu J, Black JD, Tan D and Khoury T. Epithelial-mesenchymal transition (EMT) and activated extracellular signal-regulated kinase (p-Erk) in surgically resected pancreatic cancer. Ann Surg Oncol 2007; 14: 3527-3533.

[28] Beuran M, Negoi I, Paun S, Ion AD, Bleotu C, Negoi RI and Hostiuc S. The epithelial to mesenchymal transition in pancreatic cancer: a systematic review. Pancreatology 2015; 15: 217-225.

[29] Han Z, Sergeeva O, Roelle S, Cheng H, Gao S, Li Y, Lee Z and Lu ZR. Preparation and evaluation of ZD2 peptide (64)Cu-DOTA conjugate as a positron emission tomography probe for detection and characterization of prostate cancer. ACS Omega 2019; 4: 1185-1190.

[30] Tijink BM, Perk LR, Budde M, Stigter-van Walsum M, Visser GW, Kloet RW, Dinkelborg LM, Leemans CR, Neri D and van Dongen GA. (124)I-L19-SIP for immuno-PET imaging of tumour vasculature and guidance of (131)I-L19-SIP radioimmunotherapy. Eur J Nucl Med Mol Imaging 2009; 36: 1235-1244.

[31] Eder M, Krivoshein AV, Backer M, Backer JM, Haberkorn U and Eisenhut M. ScVEGF-PEG-HBED-CC and scVEGF-PEG-NOTA conjugates: comparison of easy-to-label recombinant proteins for [68Ga]PET imaging of VEGF receptors in angiogenic vasculature. Nucl Med Biol 2010; 37: 405-412.